Effects of Substrate Temperature and Antireflection Coating on the Structural and Optical Properties of DC Sputtered Chromium Thin Films for Selective Solar Absorber Applications

Justine J Tibaijuka[1*], Margaret E. Samiji, Nuru R. Mlyuka

Physics Department, University of Dar es Salaam, P.O. Box 35063, Uvumbuzi Road Dar es Salaam Tanzania

Justine S. Nyarige, Mmantsae Diale

Physics Department, University of Pretoria, Private Bag X20, Hatfield 0028, South Africa

Abstracts

The Cr and Cr/Al_xO_y thin films were deposited by DC sputtering onto soda lime glass and polished Al substrate at various substrate temperatures. The structural analysis of the multilayered coatings revealed a weak XRD diffraction peak at 2θ≈43.3° ascribed to (110) plane of BCC structure of Cr metal, however no phase of Al_xO_y was detected due to the amorphous nature of the films. SEM and AFM analysis demonstrated the skewed distribution of small particles with an average surface roughness ranging between 3.7-13 nm. The optical analysis of the films revealed an increase in the steepness of the curve along the transition wavelength with the increase of substrate temperature, which signifies the drifting of transition wavelength towards the shorter wavelengths. Also, further lower rebounce of the reflectance curve was observed upon employing the Al_xO_y antireflection coating, indicating the drifting of transition wavelength towards the longer wavelengths. These results suggest that substrate temperature during deposition and Al_xO_y antireflection coating are potential for improving the optical properties of Cr films for selective solar absorbers applications.

Keywords: Chromium, substrate temperature, selective absorbers, antireflection coating, sputtering

* Corresponding author email: *jtibaijuka14@gmail.com*; *justine.tibaijuka@udsm.ac.tz*

1. Introduction

Concentrating solar power technology (CSP), which requires an efficient selective solar absorber, is currently intensively researched as an alternative way to minimize the overdependence on limited, non-renewable and eco-unfriendly fossil fuels. Ideally, the selective solar absorber surface, which is an essential part of CSP, should absorb all spectral solar radiation falling in it and emit none in the far infrared range [1-3]. Along with solar selectivity, the selective coating should possess high hardness, structural and chemical stability, high-temperature stability, and high corrosion and oxidation resistance. Among the selective materials that have been researched for selective coating are intrinsic selective absorbers such as Cr, V_2O_5, LaB6, Fe_3O_4, Al_2O_3, ZrB_2, ZrC, TaC, HfC, SiC, ZrB_2 [4]. Most of these materials' components are found in the lanthanide group or family of transition metals characterized by multiple orbitals energy levels that are compatible with various wavelengths of visible light. [4]. DC sputtered Chromium (Cr), among the few material candidates with intrinsic spectral selectivity, has been drawing more attention from many researchers. The interest in it is due to their tunable properties that include good adhesion, high melting point, high wear and corrosion resistance, and high thermal conductivity, which are crucial for a broad and diverse range of high-temperature applications [5-7]. Furthermore, the properties of Cr thin films can be engineered to suit diverse advanced

technology device applications other than selective spectral absorption, such as photo masks, reticules and pinhole on glass substrate integrated circuits and optical beam splitters, to mention a few [8-9].

The challenge in most of the intrinsic selective absorbers, including Cr is the lack of a steep gradient of reflectance spectra on the cross-over/transition wavelength and also the occurrence of cross-over/transition at a shorter wavelength [4]. As a result, most of the radiation falling on the surface of the absorber gets lost due to reflection. On the other hand, absorbing maximum solar energy using intrinsic absorbers requires a thick layer which consequently compromises emittance. Some of these challenges can be alleviated by employing structural or compositional engineering in the lattice of these materials, such as doping with a suitable donor, which gives rise to electron plasma and serves as scattering or making composites with some other materials [4]. Furthermore, power based multilayer structure also has been suggested for tuning the structural and optical properties of Cr thin films [7]. Additionally, the spectral selectivity of DC sputtered Cr thin films can be tailored through appropriate control of the deposition conditions such as power, gas flow rates, substrate temperature and the employment of antireflection coatings (AR). Antireflection coatings are layers usually applied on the top to enhance transmission of light to the absorbing layers and also to alleviate the loss of absorbed energy from the coating surface [1]. Ideally, the antireflection coatings works basing on the principle of interference of an electromagnetic wave. Basing on literatures, most of convention AR coatings are based on oxides and fluoride materials. So far the materials such as Al_2O_3, SiO_2, HfO_2, Ta_2O_5, LaF_3, Er_2O_3, MgF_2 and NdF_3 have been researched and applied on several devices such as spyglasses, lenses, solar panels, cameras, displays and lasers. Alumina films is among the potential antireflection coating being used in several optical devices. The interest in it is driven by its feasible properties, such as full spectral transparency from ultra-violet to mid-infrared, tunable refractive index, excellent thermal and chemical stability, and good mechanical properties (Reddy et al. 2014) that are potential for selective coating applications. Most importantly, Aluminum oxide is characterized with some intrinsic selectivity and thus its combination with Cr is ideal for selective coatings. Despite the substantial progress attained in exploring the selectivety of Cr films, the influence of substrate temperature and Al_xO_y AR coating on the spectral selectivity of DC sputtered Cr thin films remain rare addressed in the diverse open literature. This paper, therefore, presents a systematic study on the influence of substrate temperature and AR coating on the spectral selectivity of magnetron DC sputtered Cr coating.

2. 0 Experimental

2.1 Sample preparation

Cr and Al_xO_y thin films were respectively prepared onto Soda lime glass (SLG) and Aluminum substrate at various substrate temperatures between 25 °C and 300 °C by DC magnetron sputtering of Cr target (99.99%) and Al target (99.99%) commercially acquired from Plasmaterials Inc. In this research, the SLG substrate was selected to assess the optical transmittance and reflectance of Cr films, while the Al substrate was chosen to evaluate the spectral selectivity of Cr thin films. Before deposition, both the SLG and Al substrates were subjected to intensive cleaning to remove dust, grease and other stacked contaminants on the substrates through ultrasonic cleaning, followed by rinsing in distilled water and ethanol before being suspended in ethanol vapour. Before deposition, the BALZERS BAE 250 coating unit used for film preparation was evacuated to a base pressure of 7.0×10^{-6} mbar using the integrated turbo-

molecular pump backed up with a rotary pump. The Cr films were sputtered at a power of 25 W and working pressure of 5.0 x 10^{-3} mbar using argon gas flowing at a rate of 15 SCCM as ascribed in Tibaijuka et al. [7]. Likewise, the Al_xO_y antireflection layers were reactively sputtered at a power of 200 W and working pressure of 5.0 x 10^{-3} mbar using argon gas flowing at a rate of 75 SCCM and Oxygen flow rate of 4.15 SCCM. Besides, the Al and Cr targets were pre-sputtered for 10 minutes to remove the target's surface contaminants and oxides before opening the shutter to begin the deposition on the substrates. During Al_xO_y deposition, the sputtering gas (Ar) was allowed to settle for five minutes; then, the reactive oxygen gas was gradually introduced into the chamber to minimize arcing.

2.2 Sample Characterization

The films' thickness was determined by Alpha step surface profiler through measuring the step created by the stacked Teflon tape on a substrate prior to deposition. The structural phase was characterized by using a Bruker D2-Phaser X-ray Diffractometer (XRD) with Cu Kα radiation 1.5405 Å wavelength at a scanning rate of 0.02° per second for the 2θ ranging from 20°-70°. The resulting phases were identified with the help of reference PDF data available in the ICDD database. The surface morphology properties were analyzed using Zeiss Crossbeam 540 Field Emission-Scanning Electron Microscopy (FE-SEM) accelerated at the voltage of 2 kV and Nanoscope IIIA atomic force microscope in tapping mode. The resulting SEM and AFM images were post-processed for grain size distribution and surface roughness using ImageJ2 [10] and WSxM 4.0 software [11], respectively. The solar transmittance (T_{sol}) and Reflectance (R_{sol}) spectra in the wavelength range of 250 - 2500 nm were measured using Perkin Elmer Lambda 1050+ UV/VIS/NIR spectrophotometer.

3 Results and discussions

3.1 XRD Analysis

Figure 1a portrays the XRD patterns of the Cr thin films and Cr films with Al_xO_y antireflection coating prepared on SLG substrates. It can be seen that there are low-intensity broad peaks due to the amorphous nature of the films. The distinct broad peak was observed at 2θ≈43.3° which can be ascribed to the (110) plane of BCC Cr films (PDF#85-1336) [12]. In contrast, no significant crystallinity peaks attributed to Al_xO_y were present for samples with Al_xO_y AR coatings. This is due to the fact that Al_xO_y usually crystallizes at higher temperatures, around 900 °C. Similar behaviour corresponding to these results was previously reported in Cr and Al_xO_y films deposited at low power and substrate temperature [1,12-13]. Besides, the Raman spectroscopy measurements on Cr/Al_xO_y) presented in Fig. 1b revealed the significant peaks at 567 cm^{-1}, which is linked to Al-O vibration modes [14]. Figure 2 illustrates the EDX spectra of the Cr/Al_xO_y films deposited on the glass substrate. The EDX spectrum analysis showed the presence of Cr, Al, and O peaks at energies of 4.0 keV, 1.5 keV and 0.52 keV, respectively, which is consistent with other literature [15]. Likewise, the other observed peaks were attributed to arise from the s glass substrate and carbon coating before taking SEM measurements. Besides, the EDX measurement demonstrates that the deposited AR–coatings composition (Al_xO_y films) were non-stoichiometry.

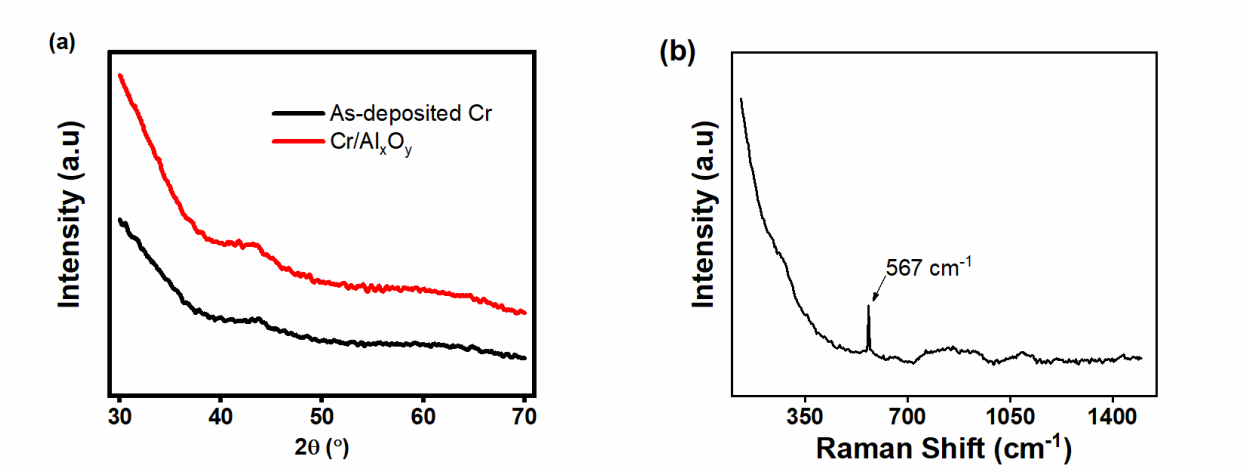

Fig. 1. The XRD spectra for as-deposited Cr layer and Cr/Al$_x$O$_y$ thin films

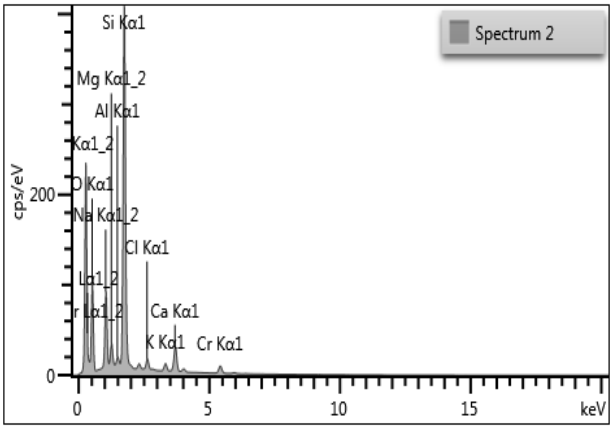

Fig. 2. EDX spectra of Cr films with Al$_x$O$_y$ AR-coating (Cr /Al$_x$O$_y$) prepared on the SLG substrate

3. 2 SEM and AFM analysis

Figures 3 and 4 shows the SEM micrograph of the Cr films prepared on SLG substrates at different substrate temperature. The film grains distribution analysis shown in Figs. 3a and 4a revealed nearly normal grains distributed for the as-deposited Cr, and the distribution skewed to the left with increased substrate temperature. Additionally, the SEM images showed the smaller grains, with an average size ranging from 5.9 to 8.1 nm and increased as the substrate temperature rose. This trend could be associated with the increased uniformity of the films with increased substrate temperature [15] as the increase in substrate temperature improves the mobility of the adatoms, thus facilitating surface diffusion and, consequently, the formation of island growth [16]. Besides, the Cr films with Al$_x$O$_y$ AR coating showed uniformly and relatively larger grains.

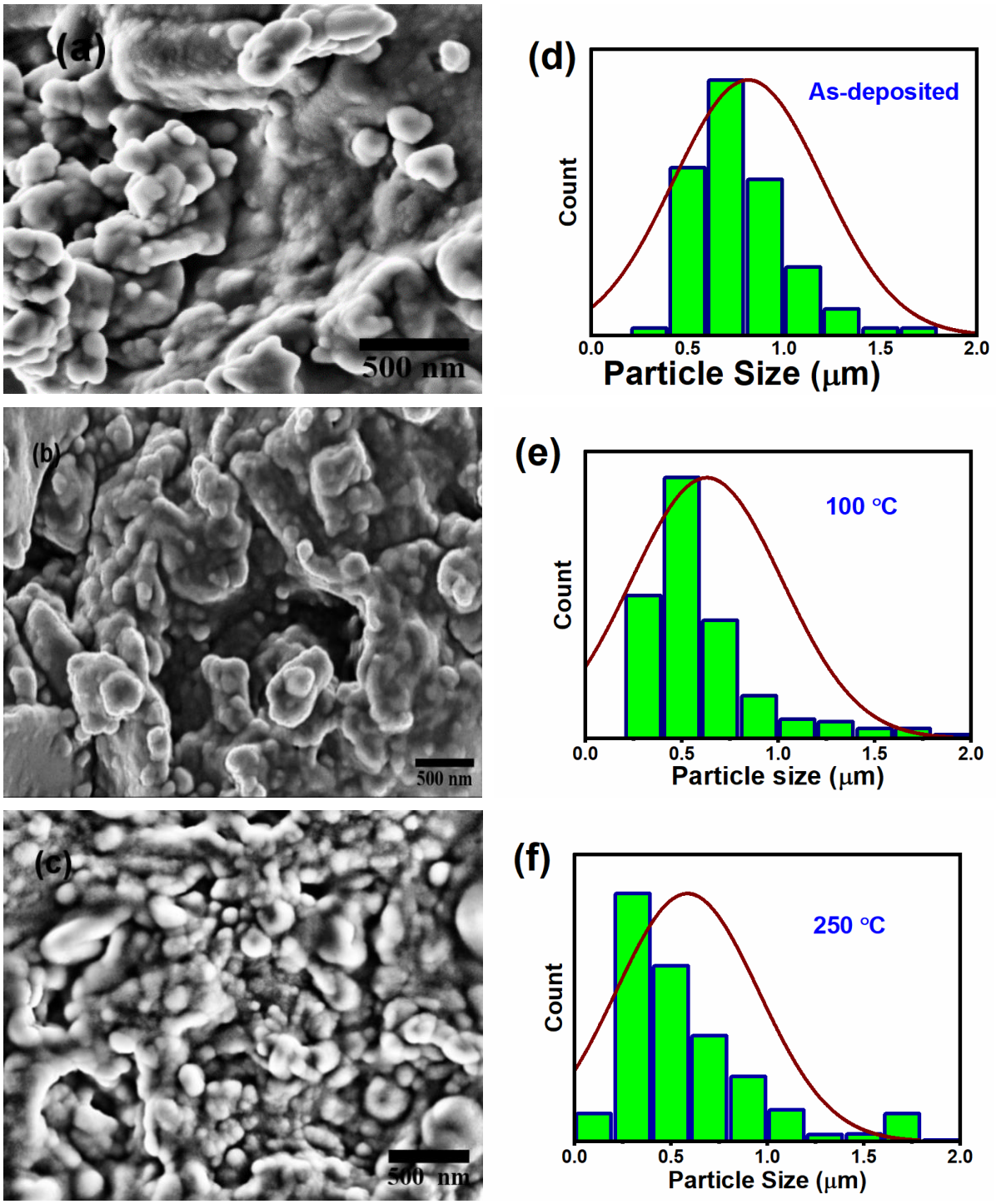

Fig. 3: SEM image and its corresponding grain size distribution for Cr films prepard on SLG at different substrate temperatures; as-deposited (a,b), 100 °C (c,d) and 250 °C (e,f).

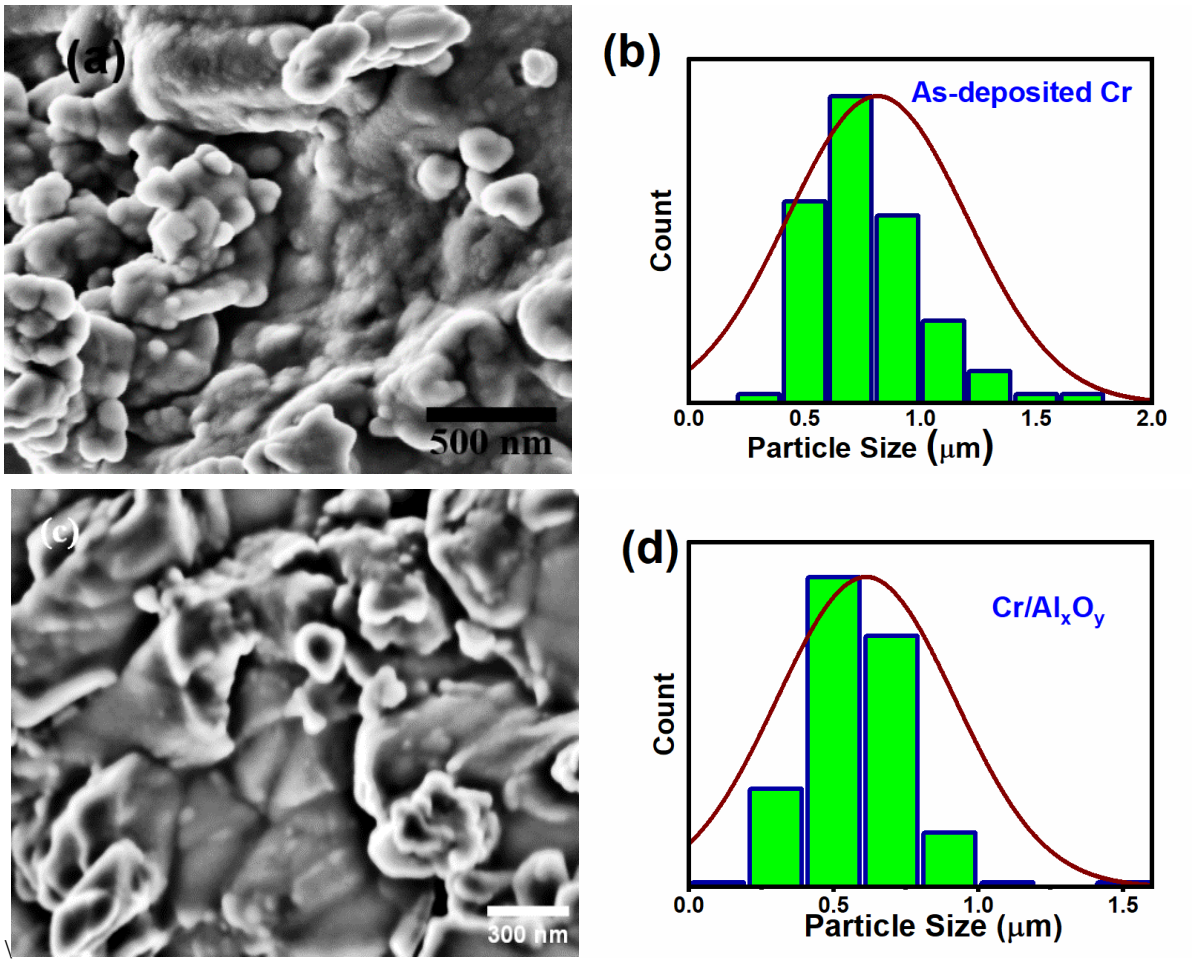

Fig 4: SEM image and the corresponding grain size distribution of the as-deposited Cr and Cr/Al_xO_y prepared on SLG.

Figures 5 and 6 present 2D and 3D AFM topographical with their corresponding height distribution for Cr and Cr/Al_xO_y films prepared onto SLG substrate. As in SEM analysis, AFM images revealed a small cluster of grains which seems to decrease with substrate temperature. Films with Al_xO_y antireflection showed uniformly and relatively larger grains, consistent with the SEM images. The results reveal further in Fig 6 the average surface roughness (Ra) and root-mean-square roughness ranging between 3.7 - 7.7 nm and 5.0 - 5.9 nm, respectively, for Cr films deposited at different substrates temperatures. No clear trend was observed in the roughness evolution with the increase in substrate temperature. Besides, Cr films with AR coating exhibited average roughness and RMS of 13 nm and 16.9 nm, respectively, which is relatively higher than their corresponding Cr films without AR coatings. The average height distribution increased with substrate temperature from 12.4 to 26.9 nm, which can be attributed to atoms migration due to substrate temperature increase, which usually facilitates the aggregation of small particles into denser grains. Besides, the average height was found to be 49 nm for Cr films with Al_xO_y AR coatings. In the characterization of the symmetry and sharpness/ peakedness of surface parameters, the height distribution analysis revealed the decrease of skewness from 3.4 to -0.9 and the spontaneous increase in kurtosis values from 0.9 to 3.4 with the increase of substrate temperature. This trend signifies the increase of peaks' sharpness and valleys on the film surface with increased substrate temperature [7,17-19]. Basing on these results, it is evident that the substrate temperature influences the

surface parameters of the films, and thus they are potential for enhancing the grains and roughness parameters of the films, which is beneficial for selective solar absorber surface engineering. Besides, the kurtosis and skewness values of 3 and 0.49, respectively, were recorded for Cr films with Al_xO_y AR coatings, indicating that broader peaks dominated the surface of the film.

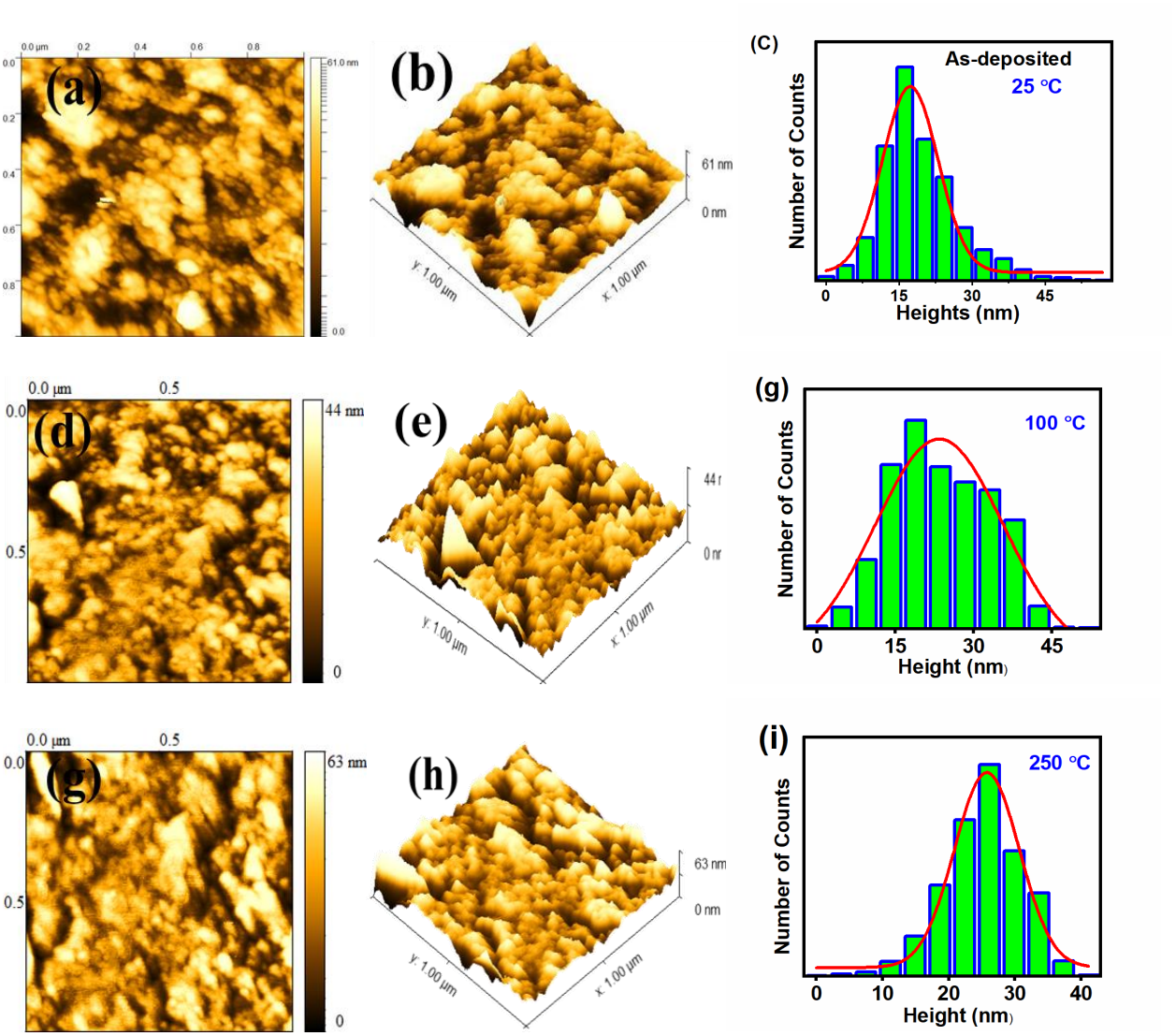

Fig. 5: 2D and 3D AFM images with the corresponding height distributions for Cr films prepared on SLG substrate at different substrate temperatures; as-deposited (a,b,c), 100 °C (e,f,g) and 250 °C (g,h,i).

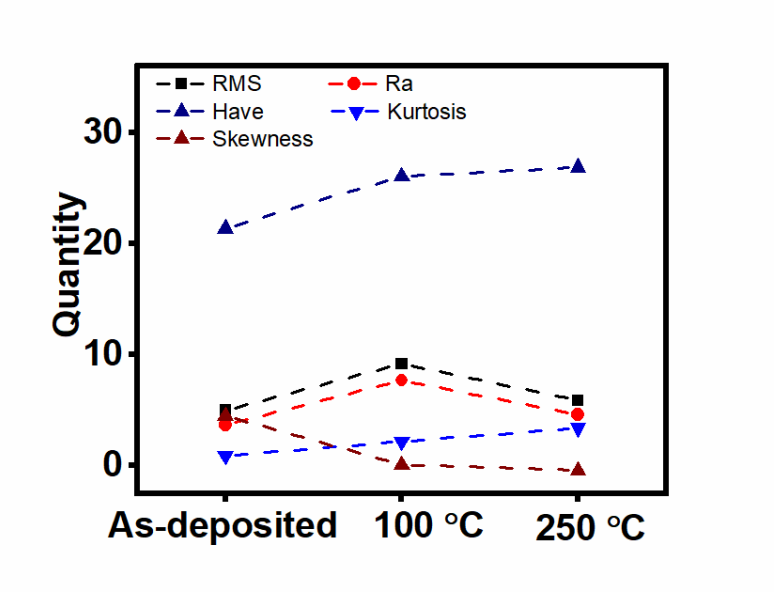

Fig. 6: AFM surface parameters for Cr prepared on SLG substrate at different substrate temperatures.

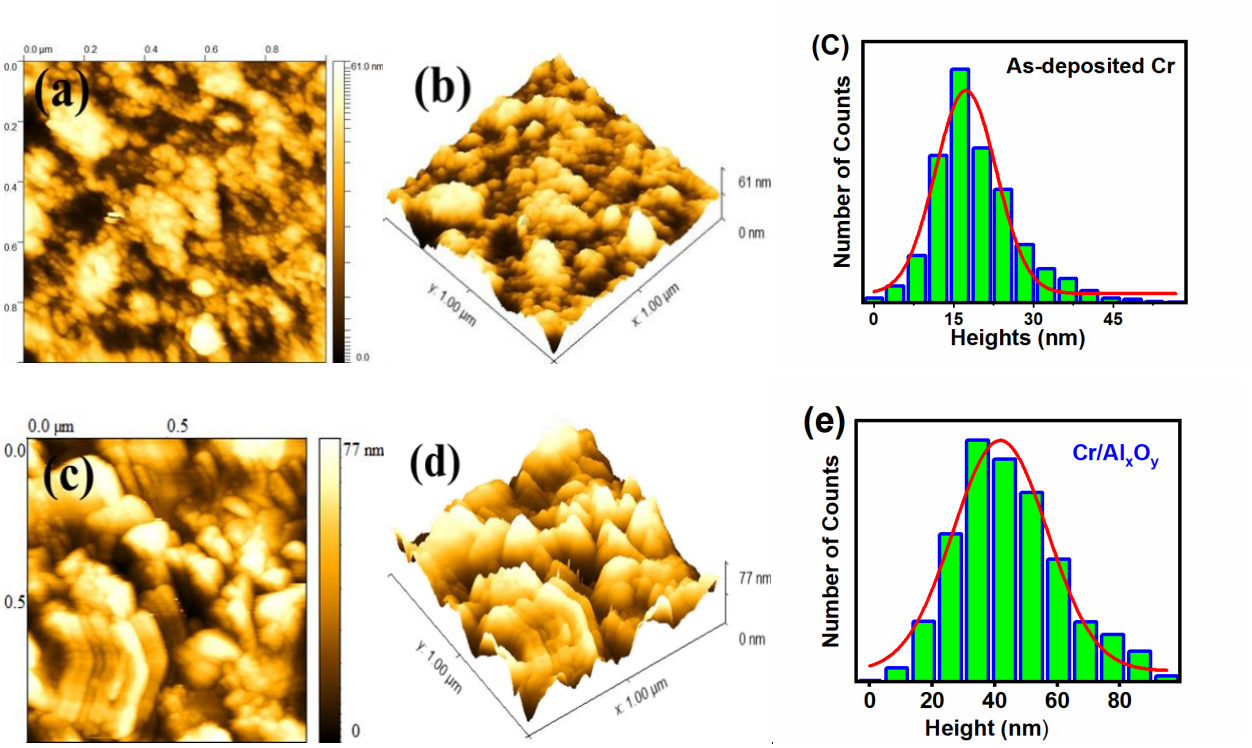

Fig. 7: 2D and 3D AFM images with corresponding height distributions for (a) as- deposited Cr films and (b) Cr/AR-coating.

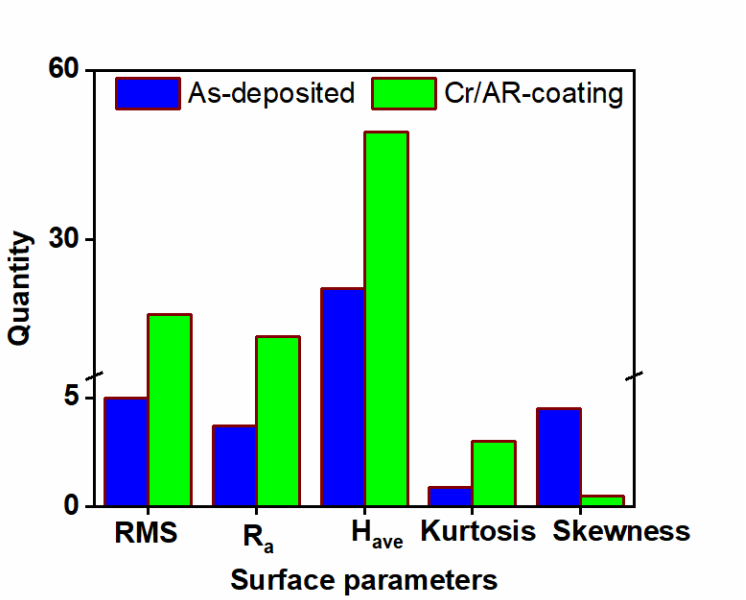

Fig. 8: AFM surface parameters for as-deposited Cr films and Cr with Al_xO_y AR-coating prepared on SLG substrates.

3. 2 Optical properties

Figure 9 shows the optical transmittances and reflectance of Cr films and Cr films with Al_xO_y prepared on glass and aluminium substrates. As reported in the previous study [7], Cr thin films on glass substrates exhibited a relatively high transmittance in the infrared region compared to the visible part in a solar spectrum. Meanwhile, the reflectance was higher in the visible spectrum and decreased gradually with the increase in wavelengths. The average transmittance (T_{ave}) was computed using equation (1) adopted from Ollotu et al. [18] at the Air Mass 1.5 solar irradiance G(λ). As shown in figure 9(a), the average transmittance was found to be ~25% while the reflectance was above 39% which are appropriate for selective solar absorber applications.

$$T_{ave} = \frac{\sum_{250}^{2500} T(\lambda)G(\lambda)}{\sum_{250}^{2500} G(\lambda)} \quad (1)$$

For the films deposited on a polished aluminium substrate, a lower reflectance rebounce curve was observed in the wavelength range of ~ 250 – 750 nm and increased abruptly in the wavelength range above 750 nm, which signifies more light is being absorbed in shorter wavelength and more light reflection in the longer wavelengths, hence spectral selectivity. Similarly, the steepness of the curve along the transition wavelength increased with the increase in substrate temperature, which indicates the drifting of transition wavelength (cross-over wavelength) towards the shorter wavelength with the increase in substrate temperature. This trend could be associated with improvement in homogeneity on the film surfaces, as revealed by the decrease of surface roughness in AFM analysis. Furthermore, the Al_xO_y antireflection coating drifted the transition wavelength (cross-over wavelength) toward the longer wavelength, signifying the improvement in spectral selectivity. With these results, it is worth mentioning that the substrate temperature and antireflection coating can enhance the selectivity of selective solar absorbers.

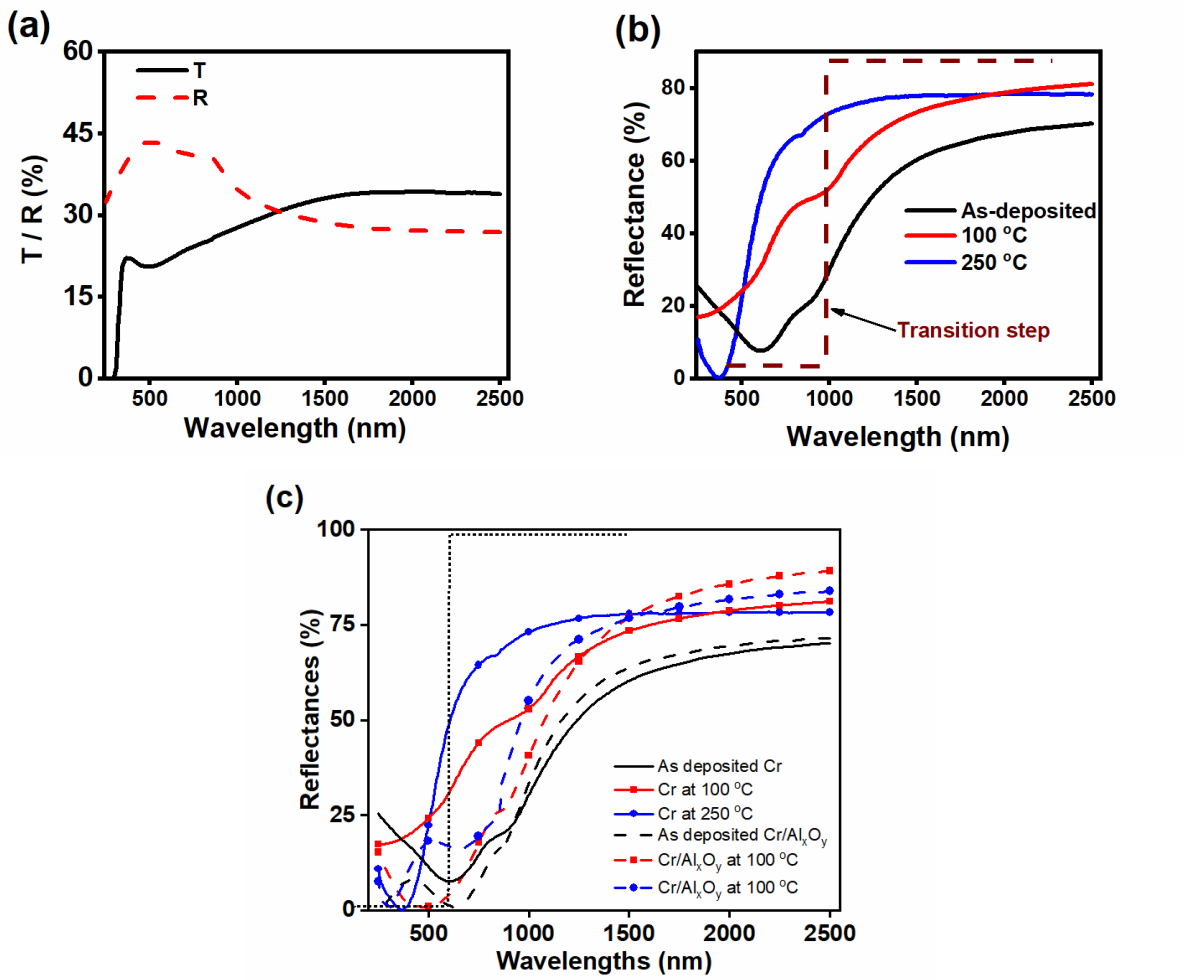

Fig. 9: Optical transmittances and reflectance of Cr films prepared on (a) SLG substrate (as-deposited), (b) Al substrate at different substrate temperatures, (c) with Al_xO_y AR coating

4. Conclusions

The Cr films and Cr with Al_xO_y AR coating were successfully fabricated through DC sputtering onto soda lime glass and polished Al substrate at various substrate temperatures. The structural analysis of the coatings revealed a low crystalline peak at $2\theta \approx 43.3°$ corresponding to (110) plane of BCC Cr films, however, no Al_xO_y diffraction peak was observed due to the amorphous nature of the films. SEM and AFM analysis revealed skewed distributed small particles with an average size of 5.9 - 8.1 nm and surface roughness of 3.7-13 nm. The optical analysis of the coating shows an increase in the steepness of the curve along the transition wavelength with the increase of substrate temperature, which signifies the drifting of transition wavelength towards the shorter wavelengths. Also, further lower rebounce of the reflectance curve was observed upon employing the Al_xO_y antireflection coating, indicating the drifting of transition wavelength towards the longer wavelengths which is desired for selective solar absorbers. These results suggest that substrate temperature during deposition and Al_xO_y antireflection coating has potential of enhancing the optical properties of Cr thin films for selective solar absorbers applications.

Acknowledgements

The Tanzanian Ministry of Education, Science, and Technology (MoEST) is sincerely appreciated for providing JT with a scholarship. The authors also acknowledge the University of Dar es Salaam, the University of Pretoria, the Materials Science and Solar Energy Network for Eastern and Southern Africa (MSSEESA), SARCHI UID No.115463, and the International Science Programme (ISP) at Uppsala University for providing research facilities and materials as well as logistical and financial support during JT lab's stay at Pretoria University.

Statements and Declarations

Conflict of Interest

The authors declare no conflict of interest.

Funding

This study was jontly supported by the Ministry of Education, Science and Technology of Tanzania (MoEST), The University of Dar es Salaam, University of Pretoria, Materials Science and Solar Energy network for Eastern and Southern Africa (MSSEESA), SARCHI UID No.115463 and the International Science Programme (ISP) - Uppsala University

Competing Interests

The authors have no relevant financial interests to disclose.

Author Contributions

All authors, except JS Nyarige contributed to the study conceptualization. Sample preparation, data collection and analysis were conducted by JJ Tibaijuka. JS Nyarige participated in SEM, Raman and XRD characterization. NR Mlyuka, M Diale and ME Samiji handled financial acquisition and supervision of work. The initial draft of the manuscript was written by Justine J Tibaijuka, and all of the other authors reviewed and edited earlier draft of the manuscript. The final manuscript was read and approved by all authors

Data Availability

Datasets related to this article data will be made available upon the reasonable request.

References

1. N. Khoza et. Al., J. Alloys Comp. (2019) https://doi.org/10.1016/j.jallcom.2018.09.329

2. A.B. Khelifa et. Al., J. Alloys Comp. (2019)
https://doi.org/10.1016/j.jallcom.2018.12.286
3. A. Al-Rjoub et. al., Sol. Energy. (2018)
https://doi.org/10.1016/j.solener.2018.04.052
4. A. Dan, H.C. Barshilia, K. Chattopadhyay, B. Basu, Ren. Sust. Energy Rev. (2017)
https://doi.org/10.1016/j.rser.2017.05.062
5. Z. Zeng, L. Wang, L. Chen, J. Zhang, Surf. Coat. Technol. (2006).
https://doi.org/10.1016/j.surfcoat.2006.03.038
6. X.Z Wang, H.Q. Fan, T. Muneshwar, K. Cadien, J.L. Luo, J. Mater. Sci. Technol. (2021)
https://doi.org/10.1016/j.jmst.2020.06.012
7. J.J. Tibaijuka, M.E. Samiji, M. Diale, N.R. Mlyuka, Tanz. J. Sci.(2022) https://dx.doi.org/10.4314/tjs.v48i3.13
8. Rauf, K. Ahmed, F. Nasim, A. N. Khan, A. Gul, IOP Conf. Ser.: Mater. Sci. Eng. (2016).
https://doi.org/10.1088/1757-899X/146/1/012013
9. J. Peralta, J. Esteve, A. Lousa,Thin Solid Films. (2020).
https://doi.org/10.1016/j.tsf.2019.137676
10. C.T. Rueden et. Al., BMC Bioinformatics. (2017)
https://doi.org/10.1186/s12859-017-1934-z
11. I. Horcas et. al., Rev. Sci. Instrum. (2007)
http://dx.doi.org/10.1063/1.2432410h
12. S.F. Wang, H.C. Lin, H.Y. Bor, Y.L. Tsai, C.N. Wei, J. Alloys Compd. (2011)
https://doi.org/10.1016/j.jallcom.2011.08.052
13. Z.Y. Nuru, C.J. Arendse, T.F.G. Muller, M. Maaza, Mater. Sci. Eng.: B. (2012)
https://doi.org/10.1016/j.mseb.2012.05.028
14. T. Sudare, Cryst. Eng. Comm. (2019)
https://doi.org/10.1039/C9CE01064E
15. ZY Nuru et. Al., Renew. Energ., 75 (2015) 590-597.
https://doi.org/10.1016/j.renene.2014.10.050.
16. R. Balu, A.R. Raju, V. Lakshminarayanan, S. Mohan, Mater. Sci. Eng.: B.(2005)
https://doi.org/10.1016/j.mseb.2005.06.021
17. O. Malik, F.J. De la Hidalga-Wade, J. Mater. Res. (2015)
https://doi.org/10.1557/jmr.2015.159
18. E.R. Ollotu, J.S. Nyarige, N.R. Mlyuka, M.E. Samiji, M. Diale, J. Mater. Sci. Mater. Electron. (2020)
https://doi.org/10.1007/s10854-020-04192-y
19. J.J. Tibaijuka, J. S. Nyarige, M. Diale, N.R. Mlyuka, M.E. Samiji, J. Mater. Sci. Mater. Electron. (2023)
https://doi.org/10.1007/s10854-022-09571-1

20. M. Szindler, M.M. Szindler, J. Orwat, G. Kulesza-Matlak, Opto-Electron Rev. (2022). https://doi.org/10.24425/opelre.2022.141952